IEEE Access
Multidisciplinary | Rapid Review | Open Access Journal

Received April 10, 2018, accepted May 24, 2018, date of publication May 31, 2018, date of current version June 20, 2018.

Digital Object Identifier 10.1109/ACCESS.2018.2842687

Radar HRRP Target Recognition Based on Concatenated Deep Neural Networks

KUO LIAO[1], JINXIU SI[1], FANGQI ZHU[2], AND XUDONG HE[1]

[1]School of Information and Communication Engineering, University of Electronic Science and Technology of China, Chengdu 611731, China
[2]Department of Electrical Engineering, University of Texas at Arlington, Arlington, TX 76010, USA

Corresponding author: Kuo Liao (liaokuo@uestc.edu.cn)

ABSTRACT In this paper, a deep neural network with concatenated structure is created for the recognition of flight targets. Compared with the traditional recognition method, the deep network model automatically gets deeper structure information that is more useful for the classification, and the better performance of target recognition is also obtained when using high-resolution range profile for radar automatic target recognition. First, the framework is expanded and cascaded by multiple shallow neural sub-networks. Then, a secondary-label coding method is proposed to solve the target-aspect angle sensitivity problem. The samples are divided into sub-classes based on aspect angle, each of which is assigned a separate encoding bit in category label. Finally, the recognition results of multiple samples are fused by a multi-evidence fusion strategy for the improvement of recognition rate. Furthermore, the effectiveness of the proposed algorithm is demonstrated on the measured and simulated data.

INDEX TERMS HRRP, deep network model, concatenated network, secondary-label, multi-evidence fusion.

I. INTRODUCTION

Radar automatic target recognition (RATR) refers to extracting the robust target features from the electromagnetic echo signal which is reflected from the target and received by the radar sensor, and utilizing the features to automatically recognize the target types or models. As the RATR technology plays a significant role in modern warfare, it has attracted wide researches in the past few decades [1]–[5]. Among these researches, the RATR based on high resolution range profile (HRRP) is a promising approach.

The HRRP is the amplitude of the echo summation for target scattering centers in each range cell of wideband radar. It reflects the distribution of target scattering centers along the radar line-of-sight (LOS), and contains the target geometric structure information that facilitates classification. Also, it has relative small dimension of data and easy to obtain. Hence, the radar target recognition based on HRRP has been intensively focused by RATR community [6]–[22]. Li and Yang [12] use HRRP as the feature vectors for data representation, and establish a decision rule based on the matching scores to identify five kinds of aircrafts. In [14], Zhou *et al.* proposed a HRRP-based radar target recognition fuzzy optimization transformation method. The goal of this approach is to maximize the distance between classes while maintaining the structure of the class. In [15], Fu *et al.* utilized the discriminant information analysis method for radar HRRP recognition. But the computation cost is too high, which does not satisfy the requirements of the approximate real-time target recognition. Zhou [17] investigated a reconstruction discriminant dictionary learning algorithm based on sparse representation classification criteria for radar target HRRP identification. Extensive experimental results demonstrate that the algorithm outperform other similar type methods like K parameters of singular value decomposition (KSVD) and discriminative dictionary learning (DDL). Zyweck *et al.* [18] proposed some data preprocessing and subspace algorithm on HRRP recognition. In above methods, feature extraction is the most critical step. The air target features are more of the domain knowledge based on the transformation of the HRRP data, such as the subspace feature, high-order spectrum feature and differential power spectrum feature. These features are abstracted by artificial rules depended much on the practical experience and application background. As a result, the role of these features in classification is difficult to assess, and the recognition accuracy of the above mentioned literatures is limited under the controlled experiment.

In recent years, with the revival of the large-scale deep neural network and the support of the high performance computing toolkits, the deep learning technique sheds a light on the traditional RATR field. In this case, some researchers begin to

leverage the power of high-dimensional nonlinear computing to pursue a higher, more accurate and robust recognition performance [23]–[27]. Lunden and Koivunen [23] built up a deep convolution neural network (CNN) to automatically extract the targets' high-order features from HRRPs for target recognition in multistatic radar systems. The experimental results show that this method achieves good recognition even at low SNR. In [24], Cui *et al.* proposed a hierarchical recognition system (HRS) based on constrained deep information network for SAR automatic target recognition. Experimental results show that the performance of the HRS is superior to some traditional pattern recognition methods. In [26], a deep network is utilized as a novel feature extraction method for HRRP-based RATR, and the average profile is considered for establishing an effective loss function under the Mahalanobis distance criterion. In summary, compared with the traditional pattern recognition method, the deep learning method for target recognition helps to avoid overusing hand-crafted rules to abstract features, and the deep expression features of the target can be automatically obtained through feature learning. The features extracted by this method are more beneficial to classification. Thus, in this paper, by leveraging the deep learning theory and the characteristics of targets HRRP data, a concatenated deep neural networks (CDNN) model is proposed for radar target recognition based on HRRP. The advantages of this framework are three-fold:

- The CDNN is formed by connecting hidden layers of multiple shallow neural sub-networks (SNSN). These sub-networks are trained from bottom to top. On the one hand, different from the traditional stacked deep neural networks (sDNN), the original HRRP data is added in the input layer of each sub-network. It as a correction to the input of current sub-network results in better depth features extracted by the CDNN than those extracted by ordinary sDNN. On another hand, the initialization parameters of the current level sub-network are transferred from the previous level, speeding up the training of the current network and reducing the risk of the network falling into a local optimum.
- A secondary-label coding method is proposed. In this method, the samples of same target are divided into four sub-classes on basis of their aspect angle, each of which is considered as a separate category. At the same time, the four sub-classes also belong to the same main class. Hence, in a secondary-label, each sample has two class tag bits, one is sub-class tag bit and another is main class tag bit. This coding method contributes to the well solution of target-aspect sensitivity problem for HRRP.
- The multi-evidence fusion strategy is employed to fuse the recognition results of multiple samples in the decision level, with the aim of further improving the target's correct recognition rate.

The rest of the paper will be arranged as follows. In section II, the HRRP signal model and deep neural network framework will be illustrated. In section III, the experiment setting for different scenarios will be introduced. In section IV, the experiment results for each case study will be demonstrated and finally we concluded in section V.

II. TARGET RECOGNITION SYSTEM

A. HRRPS' SIGNAL MODEL AND PREPROCESSING

When the radial range resolution of wide-band radar is much smaller than the target's size, the target can be modeled as a set of independent scattering centers. A HRRP is the summations of the echo vectors from each scattering centers on the target.

Consider the radar bandwidth as B, then the radar range resolution is $\Delta r = \frac{c}{2B}$, along the radar line of sight, the target can be divided into many range cells of width Δr. Then the echo of the i^{th} cell is the echo summation of all scattering centers within this range cell, which can be expressed as:

$$\begin{aligned} x_i &= \psi_i(f) \\ &= \sum_{k=1}^{N_i} a_{i,k} \exp\left(j2\pi f \tau_{i,k}\right) = I(i) + jQ(i), \end{aligned} \tag{1}$$

where f is the radar center frequency. N_i is the number of scattering centers within the i^{th} range cell. $a_{i,k}$ denotes the intensity of the k^{th} scattering center in the i^{th} cell, which is related to the scattering center's shape. $\tau_{i,k}$ is the time of arrival (TOA) of the k^{th} scattering center in the i^{th} range cell. In practice, the amplitude vector of HRRP is applied to radar target recognition. The HRRP used in the paper is defined as:

$$\mathbf{x} = [|x_1|, |x_2|, \ldots, |x_n|]^T, \tag{2}$$

where n is the dimension of the HRRP.

When using HRRP for radar target recognition, there are several issues that need to be considered: time-shift sensitivity, amplitude-scale sensitivity, and target-aspect sensitivity of HRRP.

In the measurement, a sampling window is used to extract part of data which includes the target echo from the received radar signal. The extracted part is HRRP data. Thus, in different measurements, the position of target echo in HRRP data is not fixed, which is referred to as time-shift sensitivity. The amplitude scale of HRRP varies with many factors, such as measurement environment, target distance, radar working parameters and so on. It is amplitude-scale sensitivity. In the radar line-of-sight, with the variation of target aspect, the relative position of the target scattering centers get changed and some scatters even move through different range cells. These will lead to a variation of target echo waveform, which is called target-aspect sensitivity. Therefore, to improve recognition performance, the three sensitivities should be taken into account when using HRRP for target recognition.

In preprocessing, a center alignment method is adopted for overcoming the time-shift sensitivity. On an input original HRRP data, the position of its maximum amplitude is set as the center, and $\lfloor M/2 \rfloor$ sampling points are intercepted before and after the center. When the length of the HRRP is not enough, 0 is used to make up. So the aligned HRRP data is recorded as $\mathbf{x} = [x_1, x_2, \ldots, x_M]^T$ where M is

HRRP's dimension. Then the energy normalization to each aligned HRRP is adopted to resolve amplitude-scale sensitivity. Finally, to respond to the target-aspect sensitivity, a method of embedding secondary-label in depth models is put forward, which will be described in section B_2.

B. HRRP TARGET RECOGNITION BASED ON CDNN

After the above preprocessing, the deep neural network (DNN) model is constructed to automatically extract the high-order abstract features of the target. The deeper the network, the stronger the expressive ability of the features extracted from the network is. However, the problems such as gradient vanishing and exploding and overfitting may occur during the training process, resulting in poor generalization of the model. Therefore, the correct recognition rate of the whole system cannot be improved merely by deepening the network depth. In addition, if the parameters of the neural network model are randomly initialized, the model may be trapped in local optima. In this case, a novel concatenated deep neural network structure is proposed to solve these problems.

In the CDNN, a number of independent shallow neural sub-networks (SNSN) with same structure are established, which is shown in Figure 1. These sub-networks are concatenated as a deeper network to extract the deeper features from the HRRP raw data. The input of the current sub-network is a fusion of the original HRRP data and the sample's depth features extracted from the previous sub-network. The original HRRP data is regarded as a regularization term and utilized to correct the deviation during the training, so that the better deep features can be obtained.

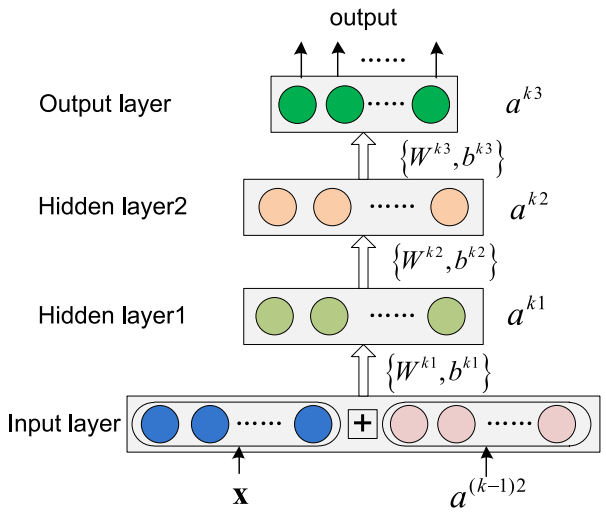

FIGURE 1. The k^{th} Shallow Neural Sub-network's Structure (SNSN_K).

1) FRAMEWORK OF SHALLOW NEURAL SUB-NETWORKS

We define the k^{th} shallow neural sub-network's structure as SNSN_K. Each sub-network is a four-layer shallow neural network consisting of an input layer, two hidden layers, and an output layer, where $W^{k1} \in \mathbb{R}^{n_1 \times n_0}$, $W^{k2} \in \mathbb{R}^{n_2 \times n_1}$, and $W^{k3} \in \mathbb{R}^{n_3 \times n_2}$ represent the weight matrix; b^{k1} , b^{k2}, and b^{k3} stand for biased vectors; the superscript $k = 1, 2, \ldots K$ represents the index of sub-networks. The number of sub-networks is set as 3 in this paper. n_0 is the dimension of the input layer, n_1 and n_2 correspond to the number of neurons in two hidden layers. n_3 is the number of node in output layers.

The input layer data is spliced by vector $\mathbf{x}$ and vector $\mathbf{a}^{(k-1)2}$, which is denoted as: $\bar{\mathbf{x}} = \left[\mathbf{x}; a^{(k-1)2}\right] = \left[x_1, x_2, \ldots, x_M, a_1^{(k-1)2}, a_2^{(k-1)2}, \ldots, a_{n_2}^{(k-1)2}\right]^T \in R^{1 \times n_0}$, where $\mathbf{x} = [x_1, x_2, \ldots, x_M]^T$ is the HRRP data after pre-processed, and M is the data dimension. $a^{(k-1)2}$ is the output vector of the second hidden layer in the previous sub-network (the $(k-1)^{th}$ sub-network), and its dimension is n_2 . So, the input layer's dimension in the sub-network is $n_0 = M + n_2$ and the output vectors of the two hidden layers are denoted as a^{k1} and a^{k2}, where

$$a^{k1} = \sigma\left(W^{k1}\bar{\mathbf{x}} + b^{k1}\right), \tag{3}$$

$$a^{k2} = \sigma\left(W^{k2}a^{k1} + b^{k2}\right). \tag{4}$$

The rectified linear unit (ReLU) functions $\sigma(z) = \max\{0, z\}$ is adopted as the activation function for the two hidden layers. The output layer uses the sigmoid activation function $f(z) = \frac{1}{1+e^{-z}}$, so the output vector of the output layer nodes is:

$$a^{k3} = f\left(W^{k3}a^{k2} + b^{k3}\right). \tag{5}$$

The cross-entropy will be set up as the cost function of the sub-network:

$$\text{Cost} = -\frac{1}{n}\sum_{j=1}^{n}\sum_{i=1}^{n_3}\left[y_i \ln a_i^{k3} + (1-y_i)\ln\left(1-a_i^{k3}\right)\right], \tag{6}$$

where $\mathbf{y} = \left[y_1, y_2, \ldots, y_{n_3}\right]^T$ represents the expected output vector, which is the real label of the input sample. $a^{k3} = \left[a_1^{k3}, a_2^{k3}, \ldots, a_{n_3}^{k3}\right]^T$ is the actual output vector of the output layer, and n is the number of training set samples.

2) SECONDARY-LABEL DESIGN

When the traditional neural networks are used for multi-classification problems, the number of nodes of the output layer is generally set as the number of target categories, and the samples' labels are coded using one-hot encoding. However, due to the target-aspect sensitivity of the HRRP, the larger the span of the samples' aspect angle, the more easily the system recognition accuracy will be reduced. Therefore, to reduce the impact of target-aspect sensitivity on the recognition system, a new coding method embedding secondary-label in the output layer of neural network is proposed.

As the target HRRP sample set is continuously sampled during the flight of the aircraft, the target-aspect of each HRRP sample is gradually changed. For the training sample set of the i^{th} target, the samples are divided into four separate subsets based on their order of sampling, each of

which corresponds to a certain aspect range of the target. A sample $\mathbf{x}^{ij}$ belongs to both its main class (the i^{th} class) and subclass. Thus, each class is assigned a secondary-label with five encoding bits. One is used to represent its main class and the other four are to represent its four subclasses. As shown in Figure 2, the middle encoding position is the main-category encoding bit.

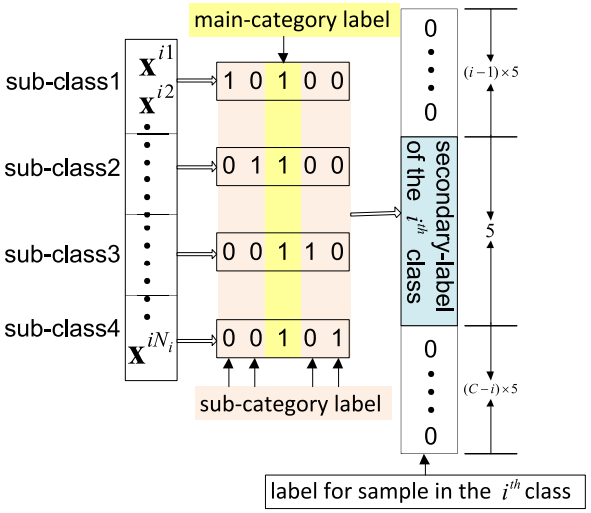

FIGURE 2. Example of encoding a sample of the i^{th} class using the secondary-lable coding method.

If there are C category targets in a recognition system, the category label of a sample consists of a series of secondary-label of these C category targets. Hence, the dimension of the sample's label is $C \times 5$. The number of neuron nodes in the sub-network output layer is $n_3 = C \times 5$. In this paper, the number of target category is $C = 4$, so the dimension of sample's label is 20. For example, if a training sample $\mathbf{x}$ belongs to the 4^{th} subclass of the 2^{nd} target, its category label is defined as:

$$\mathbf{y} = [0, 0, 0, 0, 0,\ \ 0, 0, 1, 0, 1,\ \ 0, 0, 0, 0, 0,\ \ 0, 0, 0, 0, 0].$$

3) CONCATENATION DEEP NEURAL NETWORKS

The hidden layers of each shallow neural sub-network are connected in turn to construct a CDNN. The number of sub-networks in a CDNN is determined by the actual application. By observing of the experimental results, we found that on our dataset, the best identification performance is achieved when the number of sub-networks is 3. Figure 3 shows the HRRP target recognition system framework based on CDNN network architecture that used in this paper.

The upper part of Figure 3 shows the training process of each sub-network. Each sub-network in the CDNN network is trained from bottom to top and step by step.

First, we train the bottom sub-network SNSN_1. The input layer data of this sub-network is a vector concatenated by pre-processed HRRP data $\mathbf{x} = [x_1, x_2, \ldots, x_M]^T$ and vector a^{02}, where a^{02} is the random initialized data that obey the $N(0, 1)$ distribution. Parameter set $\theta_1 = \{W^{11}, b^{11}, W^{12}, b^{12}, W^{13}, b^{13}\}$ is initialized at random. Based on the secondary-label of the sample, we utilize the stochastic gradient descent to optimize the parameter set θ_1.

After the training of sub-network SNSN_1, the second sub-network SNSN_2 is trained. The input layer data of SNSN_2 is concatenated by pre-processed HRRP vector $\mathbf{x}$ and the output vector a^{12} of the second hidden layer of SNSN_1, that is $\bar{\mathbf{x}} = [\mathbf{x}; a^{12}]$. In the process of network's parameters training, the idea of model parameter transfer is adopted in the algorithm; in other words, the trained parameters of the $(m-1)^{th}$ sub-network are passed to the m^{th} sub-network as its initial network parameters. This process not only speeds up the training of the current sub-network but also reduces the risk of the entire network falling into a local optimum. Therefore, we use the trained parameters set θ_1 to initialize the parameter set θ_2 of the sub-network SNSN_2, and utilize the stochastic gradient descent to optimize the parameter set θ_2.

The same way as mentioned above can be used to complete higher-level sub-network construction and parameter training.

The lower part of Figure 3 shows the structure of the CDNN recognition system. the final CDNN contains six hidden layers, and each hidden layer's parameters derived from three well-trained sub-networks. The output layer of CDNN is a n_3 dimensions secondary-label vector, recorded as: $\hat{y} = [\hat{y}_1, \hat{y}_2, \ldots, \hat{y}_{n_3}]^T$. In this paper, the targets' number of our recognition system is $C = 4$, so $n_3 = C \times 5 = 20$.

A decision layer is added at back of the secondary-label output layer. Firstly, the decision layer normalizes the label vector $\hat{y}$ which is predicted by the output layer:

$$\hat{\hat{y}}_i = f(\hat{y}_i) = \frac{e^{\hat{y}_i}}{\sum_{i=1}^{n_3} e^{\hat{y}_i}} \quad i = 1, 2, \ldots, n_3. \tag{7}$$

Secondly, we sum the values of the 5 encoding bits corresponding to each type of target in the secondary-vector respectively:

$$z_j = \sum_{i=(j-1)\times 5+1}^{j\times 5} \hat{\hat{y}}_i, \tag{8}$$

Finally, the output vector of the decision layer is expressed as: $\mathbf{z} = \{z_j | j = 1, 2, \ldots, C\}$. Where, z_j represents the probability that the current sample belongs to the j^{th} target. Then we predict the test sample as the p^{th} class by the maximum probability criterion, that is:

$$p = \arg\max_j \{z_j\}. \tag{9}$$

4) TARGET RECOGNITION BASED ON MULTI-EVIDENCE FUSION (MEF)

In practical applications, radar can continuously sample a series of HRRP data of the target. Using CDNN, the recognition result of each HRRP sample is obtained in real time. The accuracy of the recognition result will be further improved when the recognition results of multiple samples are fused

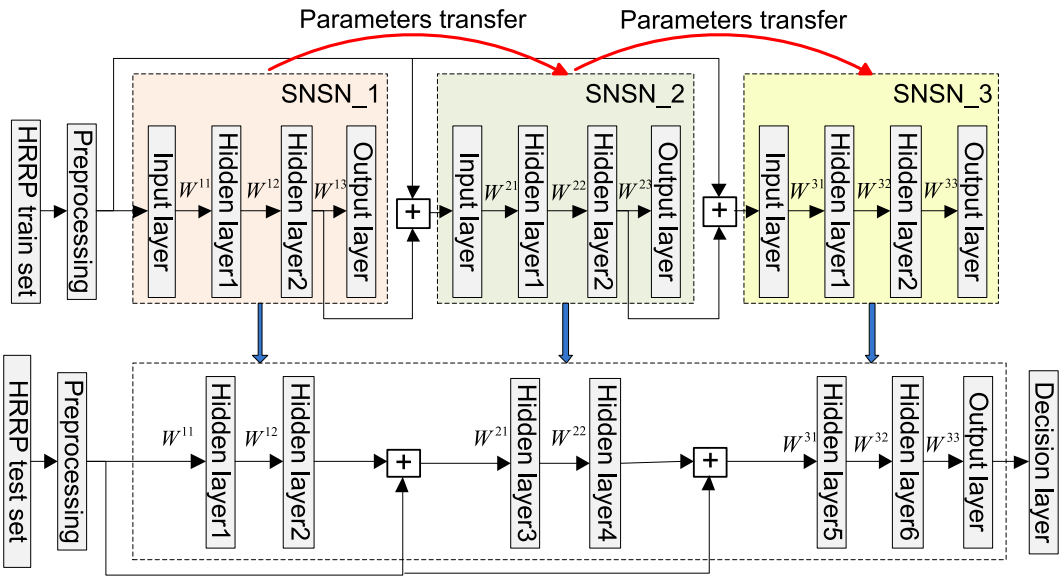

FIGURE 3. A HRRP target recognition system framework based on CDNN network architecture.

at the decision layer. For this reason, we adopt a multi-evidence fusion strategy for the CDNN identification results of D HRRP samples. In our experiment $D = 3$.

Let $\{\mathbf{x}^1, \mathbf{x}^2, \ldots, \mathbf{x}^D\}$ represents the D HRRP samples of one target. Using the CDNN to identify each sample, we can get set $\{\mathbf{z}^1, \mathbf{z}^2, \ldots, \mathbf{z}^D\} \in R^C$ containing D output vectors. Where $\{\mathbf{z}^1, \mathbf{z}^2, \ldots, \mathbf{z}^D\}$ are regarded as D independent evidences. Then the multi-evidence fusion strategy is:

$$m(j) = \sum_{p\neq q}^{D}{}_{p,q=1} z^p(j) \cdot z^q(j) \quad j = 1, 2, \ldots, C. \tag{10}$$

Where, the $z^p(j)$ represents the probability of the p^{th} sample is judged as the j^{th} class, $m(j)$ represents the probability that the test samples belongs to the j^{th} class after fusing D piece of evidences. The vector $\mathbf{m} = [m(1), m(2), \cdots, m(C)]$ is the fusion identification result. The class corresponding to the maximum probability value in vector $\mathbf{m}$ is the predicted target category, that is:

$$class_{MEF} = \arg \max_{j=1,2,\ldots,C} \{m(j)\}. \tag{11}$$

III. EXPERIMENTAL DATA AND SETTING

To verify the effectiveness of the recognition system proposed in this paper, the simulation data and measured data are used for test. At the same time, we compare our method with some traditional pattern recognition methods and general neural network recognition methods.

A. DATA DESCRIPTION

The simulation data is generated by the radar target backscatter simulation software [28], [29]. The parameters of 4 types of aircraft and radar working parameters used in the simulation experiment are shown in Table 1. The range of target aspect angle is $0^\circ \sim 180^\circ$. HRRP data is sampled at every 0.1° aspect angle, and each target class contains 1800 HRRP samples. We repeat 9 time shift operations for each sample, and the number of shifting points per time is randomly generated between -15 and 15. So, the number of samples for each class is extended to 18000. In the experiment, 70% of the samples in each category were randomly selected for model training, and the remaining 30% of the samples were used for testing. Meanwhile, the Gauss white noise with 16dB signal-to-noise ratio is added to all the simulation data.

TABLE 1. The parameters of aircrafts and radar working in simulation experiments.

Radar parameters	Center frequency Bandwidth Sampling frequency	5520 MHz 400 MHz 800 MHz
Planes	Length(m)	Width(m)
F-15	19.43	13.05
B-52	49.50	56.40
B-1B	44.80	23.80
An-26	23.80	29.21

The measured data was acquired by a self-developed wide-band radar system, and the radar's bandwidth is 200MHz. The radar is used to obtain HRRP data on four types of civilian aircraft, and the model are: Airbus A319, A320, A321 and Boeing B738. Each type of aircraft has five sets of flight data sampled at different time periods, and their route are roughly the same. In the five flight data, three sets of data are combined to form a training dataset, and the remaining two sets are fused together to serve as the testing dataset. Table 2 shows the number of samples of the measured data for each aircraft.

Figure 4 shows examples of HRRP data for simulated aircraft targets and measured aircraft targets.

TABLE 2. The number of samples of aircraft measured data.

Planes	A319	A320	B738	B321
Number of train samples	8850	7975	8590	7205
Number of test samples	6157	5452	5912	5961

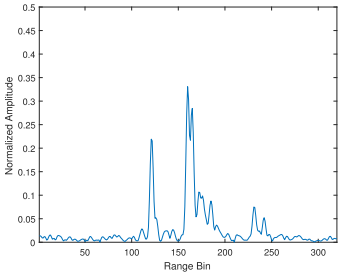

(a)

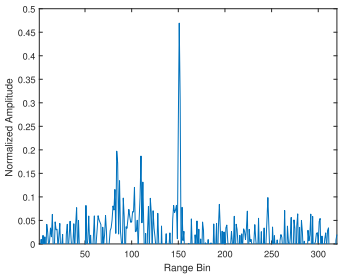

(b)

FIGURE 4. The HRRP samples of measured data and simulation data. (a) HRRP sample of measured data B738. (b) HRRP sample of simulation data F15 with 16dB White Gaussian Noise.

B. EXPERIMENTAL METHOD

To verify the effectiveness of this recognition system, three groups of comparative experiments are designed.

Experiment 1 (Verify the Effectiveness of Using CDNN for Feature Extraction): In the experiment, different numbers of SNSN are concatenated to form CDNN and the number of SNSN changes from 1 to 3. Test these different depth networks separately. The input data of the recognition system is original HRRP data, and the dimension of HRRP is $M = 320$. The number of nodes in the two hidden layers of the sub-network is set to $n_1 = 100$ and $n_2 = 50$, thus the number of nodes in input layer of the sub-network is $n_0 = M + n_2 = 370$. The traditional one-hot coding method is used to label HRRP sample. In this experiment, the number of target category is 4, thus the number of output layer's node in sub-network is $n_3 = 4$.

Moreover, the CNN and DNN recognition systems are used for the comparison experiments. The structure and parameters of CNN and DNN network are set based on Table 3. The parameters of these networks are randomly initialized and the learning rate is set as 0.1. The stochastic gradient descent method is used to train the CNN and DNN.

Experiment 2 (Verify the Effect of the Secondary-Label on Recognition Accuracy): Keep the same network structure as in Experiment 1, and change the output layer's label of each SNSN network in CDNN to the proposed secondary-label.

TABLE 3. Structure parameters of neural network recognition systems.

Network parameters of CNN	Network parameters of DNN
Input: 1*320 node	Input: 1*320 node
Conv1: 32*1*10 (st: 1,pad 1, RELU)	Hidden 1: 150 node
Pool1: 5*1 (st:, Max-pooling)	Hidden 2: 50 node
Conv2: 64*1*10 (st: 1,pad 1, RELU)	Hidden 3: 150 node
Pool2: 2*2 (st:1, Max-pooling)	Hidden 4: 50 node1
Conv3: 128*1*10(st: 1,pad 1, RELU)	Hidden 5: 150 node
Fc: 1024 node	Hidden 6: 50 node
Fc: 1024 node	softmax: 4 node
Fc: 100 node	
Softmax: 4 node	
Output: Discriminant probability vector	Output: Discriminant probability vector

Therefore, the number of output layer nodes in each SNSN is $n_3 = C \times 5 = 20$. The decision layer is added to the final layer of the system, and the entire CDNN structure is shown in Figure 3. At the same time, the output layers of the DNN and CNN in Experiment 1 are also altered accordingly and the decision layer is added to the last.

Experiment 3 (Verify the Performance of Multi-Evidence Fusion): The CDNN model with the secondary-label method proposed is used to obtain the identification result of each HRRP sample. Then the multi-evidence fusion strategy is employed to fuse the recognition results of continuous D samples of the same target, where $D = 3$.

IV. EXPERIMENTAL RESULTS AND ANALYSIS

First of all, the above three groups of experiments are implemented on the simulated HRRP data. The statistical results of the correct recognition rate are shown in Table 4. Among them, the 'CDNN_1 ', 'CDNN_2' and 'CDNN_3' represent that the number of the cascaded shallow sub-networks is 1, 2 and 3, respectively. The 'BL' stands for this method using a secondary-label, and the 'MEF' indicates use multi-evidence fusion. 'ARR' is the average correct recognition rate of four class targets.

We found the following results from Table 4:

1) As the number of cascaded sub-networks is added, the correct recognition rate of the system gradually increases. The ARR of CDNN_3 is 15.5% higher than CDNN_1, and CDNN_3_BL is 15.3% higher than CDNN_1_BL. It means that the CDNN structure is able

TABLE 4. The recognition accuracy on the simulation data by neural networks with different structure (%).

Method	An-26	F-15	B-52	B-1B	ARR
DNN	82.1	88.1	91.5	89.3	87.7
CNN	86.6	93.2	95.4	92.1	91.8
CDNN_1	74.3	80.0	83.6	77.3	77.9
CDNN_2	90.2	82.7	87.3	91.6	88.0
CDNN_3	93.7	91.2	92.5	96.2	93.4
DNN_BL	90.4	95.2	93.1	87.7	91.6
CNN_BL	86.3	96.3	97.5	95.6	93.3
CDNN_1_BL	75.6	79.2	81.7	85.9	80.6
CDNN_2_BL	88.0	93.1	94.4	94.3	92.5
CDNN_3_BL	94.3	97.7	96.4	95.2	95.9
CDNN_3_BL_MEF	96.2	98.1	97.2	98.5	97.5

to abstract the deep distinguishing features of the target. Compared with shallow features, the deep features have more excellent classification performance.

2) The classification ability of CDNN is better than that of an ordinary depth model with the same depth. The CDNN_3 model has 6 hidden layers, basically the same as the number of hidden layers in the DNN and CNN networks used in comparison experiments. The recognition rate of CDNN_3 is 1.6% higher than the DNN and CNN networks at least. This result indicates that compared with the ordinary deep network structure, the proposed network structure abstracts more effective depth distinguish features for target recognition.
3) With the use of secondary-label method, the average recognition accuracy of various recognition methods increases by at least 1.5%. This demonstrates that the secondary-label method can alleviate the impact of HRRP aspect-sensitivity on recognition, and the extracted features are more robust to the aspect change of the target.
4) Using multi-evidence fusion strategy, the average correct recognition rate of CDNN_3_BL_MEF reaches 97.5%, 1.6% higher than that of a single sample.

To further verify the performance of the proposed algorithm, the measured data is employed to repeat the above experiments. In the mean time, the traditional pattern recognition methods such as SVM, LDA and PCA are used for comparative experiments. The correct recognition rate of all methods is shown in Table 5.

TABLE 5. The recognition accuracy on the measured data by various identification methods (%).

Method	B738	A320	A319	A321	ARR
PCA	74.0	87.3	97.0	61.2	79.9
LDA	74.2	80.8	96.1	75.0	81.5
SVM	74.0	84.8	96.2	79.0	83.5
DNN	78.6	85.3	100.0	83.2	86.8
CNN	82.0	86.7	100.0	83.3	87.8
CDNN_3	81.3	84.8	100.0	86.4	88.1
CDNN_3_BL	84.6	87.9	100.0	85.7	89.6
CDNN_3_BL_MEF	87.5	93.8	100.0	88.9	92.5

Experimental results based on measured data also reveal that the traditional PCA, LDA and SVM pattern recognition methods only extract the shallow features of targets, and the best recognition accuracy of these methods is 83.5%. On the contrary, the deeper features of the target are extracted by deep neural network model, and the classification capability of the deep features is significantly better than that of shallow features. As shows in Table 5, the recognition accuracy of CDNN_3 model is 88.1%, 4.6% higher than that of SVM method. On this basis, by using the secondary-label and multi-evidence fusion strategy, the recognition accuracy of the CDNN_3_BL_MEF model can be increased to 92.5%.

V. CONCLUSION

In this paper, a novel deep neural network recognition system is designed and used for aircraft target recognition based on radar HRRP data. It is established by the connection of multiple shallow neural networks. As a correction to high-order features extracted, the original HRRP data is extended to the input layer of every SNSN. Hence, this concatenated deep neural network learns more effective depth features for target recognition than normal deep networks. Furthermore, a secondary-label coding method is put forward, in which the target samples are divided into different aspect zones and the samples in each zone have a separate subclass tag bit and a public main class tag bit. Training network's parameters by this secondary-label helps to reduce intra-class differences between the extracted features and increase their between-class difference. In this way, it optimizes the target clustering and alleviates the impact of target-aspect sensitivity on recognition performance. Finally, the multi-evidence fusion strategy is introduced to further improve the system recognition rate. The experimental results on simulation and measured airplanes HRRP data prove the effectiveness of the proposed CDNN recognition system. In summary, using the CDNN model proposed in this paper, we can effectively abstract the deep features of targets, that is beneficial to the classification, from aircraft target HRRP data. Meanwhile, better recognition performance than traditional recognition methods and ordinary deep learning methods is achieved.

REFERENCES

[1] B. Chen, H. Liu, J. Chai, and Z. Bao, "Large margin feature weighting method via linear programming," *IEEE Trans. Knowl. Data Eng.*, vol. 21, no. 10, pp. 1475–1488, Oct. 2009.
[2] C. R. Smith and P. M. Goggana, "Radar target recognition," *IEEE Antennas Propag. Mag.*, vol. 35, no. 2, pp. 27–38, Apr. 1993. [Online]. Available: https://ieeexplore.ieee.org/abstract/document/207649/
[3] L. Du, H. Liu, Z. Bao, and J. Zhang, "Radar automatic target recognition using complex high-resolution range profiles," *IET Radar, Sonar Navigat.*, vol. 1, no. 1, pp. 18–26, Feb. 2007.
[4] L. Du, H. Liu, P. Wang, B. Feng, M. Pan, and Z. Bao, "Noise robust radar HRRP target recognition based on multitask factor analysis with small training data size," *IEEE Trans. Signal Process.*, vol. 60, no. 7, pp. 3546–3559, Jul. 2012.
[5] S. P. Jacobs, "Automatic target recognition using high-resolution radar range profiles," Ph.D. dissertation, Washington Univ., St. Louis, MO, USA, 1997. [Online]. Available: https://dl.acm.org/citation.cfm?id=925410
[6] X.-D. Zhang, Y. Shi, and Z. Bao, "A new feature vector using selected bispectra for signal classification with application in radar target recognition," *IEEE Trans. Signal Process.*, vol. 49, no. 9, pp. 1875–1885, Sep. 2001.
[7] L. Du, H. Liu, Z. Bao, and J. Zhang, "A two-distribution compounded statistical model for radar HRRP target recognition," *IEEE Trans. Signal Process.*, vol. 54, no. 6, pp. 2226–2238, Jun. 2006.
[8] Y. Liu, D. Zhu, X. Li, and Z. Zhuang, "Micromotion characteristic acquisition based on wideband radar phase," *IEEE Trans. Geosci. Remote Sens.*, vol. 52, no. 6, pp. 3650–3657, Jun. 2014.
[9] S. P. Jacobs and J. A. O'Sullivan, "Automatic target recognition using sequences of high resolution radar range-profiles," *IEEE Trans. Aerosp. Electron. Syst.*, vol. 36, no. 2, pp. 364–381, Apr. 2000.
[10] R. Wu, Q. Gao, J. Liu, and H. Gu, "ATR scheme based on 1-D HRR profiles," *Electron. Lett.*, vol. 38, no. 24, pp. 1586–1588, Nov. 2002.
[11] L. Du, H. Liu, Z. Bao, and M. Xing, "Radar HRRP target recognition based on higher order spectra," *IEEE Trans. Signal Process.*, vol. 53, no. 7, pp. 2359–2368, Jul. 2005.

[12] H.-J. Li and S.-H. Yang, "Using range profiles as feature vectors to identify aerospace objects," *IEEE Trans. Antennas Propag.*, vol. 41, no. 3, pp. 261–268, Mar. 1993.
[13] S. K. Wong, "Non-cooperative target recognition in the frequency domain," *IEE Proc.-Radar Sonar Navigat.*, vol. 151, no. 2, pp. 77–84, 2004.
[14] D. Zhou, X. Shen, and W. Yang, "Radar target recognition based on fuzzy optimal transformation using high-resolution range profile," *Pattern Recognit. Lett.*, vol. 34, no. 3, pp. 256–264, 2013.
[15] J. Fu, X. Deng, and W. Yang, "Radar HRRP recognition based on discriminant information analysis," *WSEAS Trans. Inf. Sci. Appl.*, vol. 8, no. 4, pp. 185–201, 2011.
[16] K. B. Eom and R. Chellappa, "Noncooperative target classification using hierarchical modeling of high-range resolution radar signatures," *IEEE Trans. Signal Process.*, vol. 45, no. 9, pp. 2318–2327, Sep. 1997.
[17] D. Zhou, "Radar target HRRP recognition based on reconstructive and discriminative dictionary learning," *Signal Process*, vol. 126, pp. 52–64, Sep. 2016.
[18] A. Zyweck and R. E. Bogner, "Radar target classification of commercial aircraft," *IEEE Trans. Aerosp. Electron. Syst.*, vol. 32, no. 2, pp. 598–606, Apr. 1996.
[19] Z. Guo and S. Li, "One-dimensional frequency-domain features for aircraft recognition from radar range profiles," *IEEE Trans. Aerosp. Electron. Syst.*, vol. 46, no. 4, pp. 1880–1892, Oct. 2010.
[20] C. Mao and J. Liang, "HRRP recognition in radar sensor network," *Ad Hoc Netw.*, vol. 58, pp. 171–178, Apr. 2017.
[21] F. Zhu and J. Liang, "Air targets recognition using a fuzzy logic approach," in *Proc. IEEE 6th Int. Conf. Wireless Commun. Signal Process. (WCSP)*, Oct. 2014, pp. 1–6.
[22] J. Liang and F. Zhu, "Fuzzy logic classifier design for air targets recognition based on HRRP," *Phys. Commun.*, vol. 13, pp. 205–210, Dec. 2014.
[23] J. Lundén and V. Koivunen, "Deep learning for HRRP-based target recognition in multistatic radar systems," in *Proc. IEEE Radar Conf.*, May 2016, pp. 1–6.
[24] Z. Cui, Z. Cao, J. Yang, and H. Ren, "Hierarchical recognition system for target recognition from sparse representations," *Math. Problems Eng.*, vol. 2015, Jan. 2015, Art. no. 527095. [Online]. Available: https://www.hindawi.com/journals/mpe/2015/527095/
[25] S. Zhou, Q. Chen, and X. Wang, "Active deep learning method for semi-supervised sentiment classification," *Neurocomputing*, vol. 120, pp. 536–546, Nov. 2013.
[26] B. Feng, B. Chen, and H. Liu, "Radar HRRP target recognition with deep networks," *Pattern Recognit.*, vol. 61, pp. 379–393, Jan. 2017.
[27] O. Basir and X. Yuan, "Engine fault diagnosis based on multi-sensor information fusion using Dempster–Shafer evidence theory," *Inf. Fusion*, vol. 8, no. 4, pp. 379–386, 2007.
[28] Y. D. Shirman, *Computer Simulation of Aerial Target Radar Scattering, Recognition, Detection, and Tracking*. Boston, MA, USA: Artech House, 2002, pp. 1–315.
[29] S. A. Gorshkov, S. P. Leshchenko, V. M. Orlenko, Y. D. Shirman, and S. Y. Sedyshev, *Radar Target Backscattering Simulation: Software and User's Manual*. Boston, MA, USA: Artech House, 2002, pp. 1–17.

KUO LIAO received the B.S. degree in computer science and technology from the Chengdu University of Technology, Chengdu, China, in 2001, and the M.S. and Ph.D. degrees in electrical engineering from the University of Electronic Science and Technology of China, Chengdu, in 2004 and 2012, respectively. She is currently an Associate Professor with the Department of Information and Communication Engineering, University of Electronic Science and Technology of China. Her current research interests include radar target recognition, radar signal processing, and machine learning.

JINXIU SI received the B.S. degree from the Department of Electronic Information Engineering, Huaihai Institute of Technology, Lianyungang, China, in 2015. He is currently pursuing the M.S. degree with the School of Information and Telecommunication Engineering, University of Electronic Science and Technology of China, Chengdu, China. His current research interests include radar target recognition, pattern recognition, and deep learning.

FANGQI ZHU was born in Chengdu, China, in 1991. He received the B.S. and M.S. degrees in electrical engineering from the University of Electronic Science and Technology of China, Chengdu, in 2013 and 2016, respectively. He is currently pursuing the Ph.D. degree in electrical engineering with the University of Texas at Arlington, Arlington, TX, USA. His current research interests include machine learning, signal detection and estimation, statistical inference, and computational intelligence. He is a reviewer for several conferences and journals.

XUDONG HE received the B.S. degree from the School of Information and Communication Engineering, University of Electronic Science and Technology of China, Chengdu, China, in 2016, where he is currently pursuing the M.S. degree. His research interests include radar target recognition and pattern recognition.